On the universality class dependence of period doubling indices

Mario Feingold [a], Diego L. Gonzalez [b], Marcelo O. Magnasco [b,c] and Oreste Piro [b,c,d]

[a] *Theory of Condensed Matter, Cavendish Laboratory, Cambridge University, Cambridge, CB3 0HE, UK*
[b] *Departamento de Fisica, Universidad Nacional de La Plata, C.C. 67, 1900 La Plata, Argentina*
[c] *The James Franck Institute, The University of Chicago, Chicago, IL 60637, USA*
[d] *Center for Nonlinear Studies, MS-B 258, Los Alamos National Laboratory, Los Alamos, NM 87544, USA*

The dependence on ν of the period doubling scaling indices for unimodal maps with a critical point of the form $|x|^{\nu}$ is numerically investigated. A new symbolic dynamics based computation technique working in configuration space is introduced. The existence of an upper bound for $\delta(\nu \to \infty)$ is numerically verified. An accurate estimate of 29.8 is given for this limit. Moreover, the global functional form of $\delta(\nu)$ is shown to have an interesting symmetry.

Period doubling universality is a well established theory [1,2]. It is well known, for instance, that the scaling behavior near the onset of chaos for one-parameter families of unimodal maps of the interval, $f_{\lambda}(|x|^{\nu})$ with a critical point of order $|x|^{\nu}$ only depends on ν [3,4]. In fact, ν labels the universality classes of unimodal maps which share the same scaling behavior. In other words, the indices describing such scaling are class functionals. Since the classes are only parametrized by ν, these indices are universal functions of ν. In particular, the accumulation rate δ of the period doubling bifurcation sequence in parameter space and the scaling factor α for the highly bifurcated orbits around the critical point are both universal functions of ν [5]. In the range $\nu \in (1, \infty)$, there are two singular limits in the scaling behavior. For $\nu \to 1$ the scaling factor α diverges. This limit can be analyzed rigorously in the framework of renormalization group theory as a perturbation to the tent map. Such analysis leads to the result $\delta(\nu \to 1) = 2$. Although the validity of the result is out of question, an accurate numerical check in the configuration space of the cascade is difficult to achieve due to the divergence of $\alpha(\nu)$. At the opposite extreme, the other singular limit $\nu \to \infty$ is equally difficult to study numerically. In this case, renormali-

zation group schemes [6–9] give an upper bound of about 30 for $\delta(\nu)$.

The aim of this paper is to investigate numerically the $\nu \to \infty$ limit for $\delta(\nu)$, not in a renormalization group framework, but rather by using its real space definition as the asymptotic rate of convergence for superstable parameter values. For this purpose, we introduce a map of infinite order in the sense that all its derivatives vanish at the critical point. In order to investigate the period doubling cascades in this extremely difficult case, we developed a powerful numerical technique which we shall describe below. To test the reliability of the method, we compute the limit $\nu \to 1^{+}$ up to an accuracy never reached numerically before. Finally, we speculate about the global form of the function $\delta(\nu)$ which shows a nice symmetry.

The ratio

$$\delta = \lim_{n \to \infty} \delta_n$$

with

$$\delta_n = (\lambda_n - \lambda_{n-1})/(\lambda_{n+1} - \lambda_n)$$

as a function of the order of the maximum of f_{λ} is computed numerically by finding the superstable points λ_n which satisfy $f_{\lambda_n}^{2^n}(x_{\max}) = x_{\max}$. Similarly,

the universal scaling index α is defined as $\alpha_n = d_n / d_{n+1}$, $\alpha = \lim_{n\to\infty} \alpha_n$, where d_n is the distance from the maximum to the nearest element of the orbit. The renormalization group equation, $g(x) = -\alpha g \circ g(-x/\alpha)$, implies that $\alpha^\nu / \nu - \alpha = 1$ up to first order in a power series expansion.

Clearly, there are two singular limits: (a) $\nu \to 1$. In this limit the scaling factor $\alpha(\nu)$ diverges and accordingly, the widths of successive branches of the attractors decrease faster than exponentially with n. This behavior corresponds to the fact that in the limit the map approaches the *tent map* $(x_{n+1} = \lambda(1 - |2x_n - 1|))$ in the neighborhood of the critical point. For such maps, all λ_n collapse to a single value $\lambda_0 = \frac{1}{2}$ (i.e. the 2^n cycles appear all at once) [10] and the onset of chaos attractor shrinks to a single point in phase space. Nevertheless, it can be proven that $\delta(\nu \to 1) \to 2$ [4]. However, direct numerical computations in this limit are extremely difficult (the best result in the literature is [11] $\delta(1.1) = 2.81$). The origin of the difficulty is, of course, the divergence of $\alpha(\nu)$. (b) $\nu \to \infty$. In this limit, $\alpha(\nu)$ tends to unity. Consequently, the distance between branches in the neighborhood of the maximum scale slower than geometrically. On the other hand, although a truncated RG analysis shows a divergent $\delta(\nu)$ [12], more careful treatments [6–9] lead to an upper bound for $\delta(\infty)$. Although these arguments yield good estimates for this limit, a direct numerical calculation is again very difficult.

First of all, $\delta(\infty)$ is usually defined [8] as $\lim_{\nu\to\infty} \lim_{n\to\infty} \delta_n(\nu)$. This double limit is however singular. In fact, the sequence of maps $f_\nu = 1 - k|x|^\nu$ converges to a discontinuous function f_∞, which takes on the value of $-\infty$ for x outside of $[-1, 1]$ and 1 inside. It is clearly impossible to calculate the scaling index for the f_∞. However, since the value of δ is only sensitive to the shape of f near the maximum, we can regularize such a limit by considering the alternative family

$$g_\nu(x) = 1 - k[\,|x|^\nu + \exp(-1/x^2)\,] \ .$$

We will show that the inverted limits $\lim_{n\to\infty} \lim_{\nu\to\infty} \delta_n(\nu)$ is consistent with the expected values of $\delta(\infty)$ [8,9]. In fact, we consider the *inverse Gaussian map*

$$x_{n+1} = \lambda(1 - \exp\{-[\mu/(x_n - \tfrac{1}{2})]^2\}), \quad \text{if } x \neq \tfrac{1}{2} ,$$
$$= \lambda, \qquad\qquad\qquad\qquad\qquad\quad \text{if } x = \tfrac{1}{2} ,$$

$$(1)$$

as the $\nu = \infty$ member of a family like g_ν. This map has all derivatives continuously vanish at the maximum and is unimodal in its neighborhood.

The second difficulty arises from the fact that the derivatives of $F(\lambda) = f_\lambda^{2^n}(x_{\max}) - x_{\max}$, whose zeroes define the λ_n, increase with n as $(-\delta/\alpha)^n$. This makes standard numerical methods very inefficient. Instead, we devised an algorithm which relies on some results from the symbolic dynamics theory.

It is well known that as λ is increased the stable periodic orbits of unimodal maps appear in a universal order known as MSS [3]. The proof of this result is based on the symbolic description of trajectories. This consists of associating to each orbit of period n a sequence of n symbols R (right), L (left) or C (center), according to the position relative to the critical point of each orbit element. It can be shown that the symbolic sequences of a given periodic orbit and the one of a transient, which starts from $x_0 = x_{\max}$ are the same. Thus, by convention, the orbits always start with $x_0 = x_{\max}$, so as to avoid cyclic permutations of the sequences. Therefore, superstable orbits always end with C. The symbolic description distinguishes between orbits with $\lambda < \lambda_s$ and $\lambda > \lambda_s$ where λ_s indicates superstability.

Not all sequences of symbols correspond to allowed stable orbits (e.g. no sequences may begin with LR), the MSS work [3] leads to an algorithm for the construction of the allowed sequences corresponding to superstable orbits and also specifies the order of these orbits in parameter space. A less publicized result [13] is that the MSS order can be translated into a binary tree by means of appropriate labeling. Each node of the tree is associated with a symbolic sequence. Both allowed and forbidden sequences are present but the former are precisely in the MSS order. Thus, the tree translates the MSS order into the order of real numbers.

The labeling of the tree proceeds by associating an R or an L to each link, such that each horizontal level reads LRRLLRRL... (see fig. 1). Thus, each node represents a symbolic sequence which is obtained by reading the symbols on the corresponding chain of
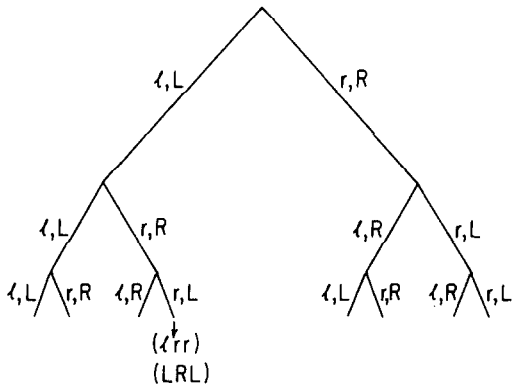
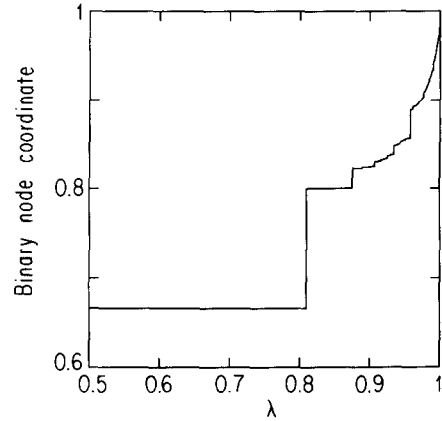Fig. 1. The binary tree with both the Gray and the binary labeling.

Fig. 2. The binary assigned node coordinates for the binary tree in fig. 1 versus the value of λ at which the corresponding periodic orbits are superstable for the logistic map ($\nu = 2$).

links from the top to the node. Note that the L symbol in this labeling indicates *continue in the same direction* while the R symbol means *reverse direction*. This labeling, known as *Gray encoding*, is an alternative to the ordinary binary labeling which indicates *absolute* left or right movements on the tree (ℓ or r in fig. 1) [14]. The labeling schemes can be interpreted in terms of the variation, ϵ_n, of the orbit, x_n, $x_{n+1} + \epsilon_{n+1} = f(x_n) + f'(x_n)\epsilon_n$. Namely, $S_n = R$ (L) if $s_n = 1$ (-1), where $s_n = \text{sign}[f'(x_n)]$. On the other hand, the sign of the ϵ_n is

$$\nu_n = \text{sign}(\epsilon_n) \equiv \prod_{i=1}^{n} \text{sign}[f'(x_n)]$$

and consequently, the ℓ, r symbols are defined as $V_n = r$ (ℓ) if $\nu_n = -1$ (1). In other words, the absolute movements on the tree can be deduced from the sign of the variation at the nth iterate.

To illustrate the result (proven in ref. [13]) that the natural order of the nodes restricted to allowed sequences coincides with the MSS order we show in fig. 2 the coordinate of the nodes which are associated with the symbolic sequences generated by the logistic map ($\nu = 2$), as a function of λ [#1]. The statement is then substantiated by the fact that the graph in fig. 2 is monotonic.

We further use the invariance of symbolic sequence of the period doubling attractor under the substitution $R \rightarrow RL$ and $L \rightarrow RR$ [#2]. This leads to the

---

[#1] The coordinate of a node is given by its binary address.

[#2] This follows from $S = R * S$, where S is the onset of chaos sequence, and $*$ is the sequence product defined by MSS.
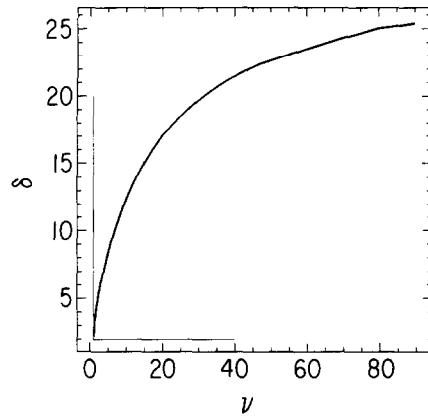

Fig. 3. δ versus ν for the range $\nu \in (1.0015, 90)$.

formula $S_i = R$ (L) if n_i is odd (even) where n_i is the maximum integer k such that 2^k divides i.

Furnished with these results, we are able to recognize whether an orbit produces a symbolic sequence which is before or after the desired superstable one. Therefore, we can devise a powerful numerical scheme to detect superstable orbits based on a simple bracketing search. This method, of course, always converges even in the singular limits mentioned above. Different symbolic dynamical algorithms to detect superstable orbits were also used by Hao [15].

The function $\delta(\nu)$ computed with this method for maps of the form $x_{n+1} = \lambda(1 - |1 - 2x_n|^\nu)$ for ν between 1.0015 and 90 is shown in fig. 3. It is clearly

seen that $\delta(\nu)$ is a smooth monotonically increasing function in agreement with the renormalization group theory [2,4].

To test the power of the numerical method, we can consider the $\nu \rightarrow 1^+$ limit. Notice that although the convergence to the theoretical result $\delta \rightarrow 2$ is very slow, we were able to compute $\delta(1.0015) = 2.2442...$ for ν, two orders of magnitude closer to one than the best numerical results previously available. Since δ still differs by more than 10% from the limit we also studied its convergence. We fitted our computed values with the expression

$$\log(\nu - 1) \approx \frac{a}{(\delta - 2)^b} + c \qquad (2)$$

for small values of $\nu - 1$. Although the additive constant c is uncertain, one can make a good estimation for b and a. In fig. 4 we have plotted $\log[-\log(\nu - 1) - c]$ versus $\log(\delta - 2)$ for several values of c. The graph becomes linear for small values of $\delta - 2$. The quality of the linear fit in this region is best for $c \approx 1.25$ and this leads to $b \approx 0.46$ which are again consistent with the behavior predicted by the renormalization group theory [4].

Let us consider now the $\nu \rightarrow \infty$ limit. At first glance, the curve $\delta(\nu)$ shown in fig. 3 could lead to the impression that this limit is $\sqrt{\nu}$-divergent. However, a more refined analysis (see fig. 6) indicates the existence of an upper bound. One could clarify this by computing δ for increasingly higher (but finite) values of ν but this approach becomes impractical above $\nu \approx 100$. Instead, we compute it for the map in eq.
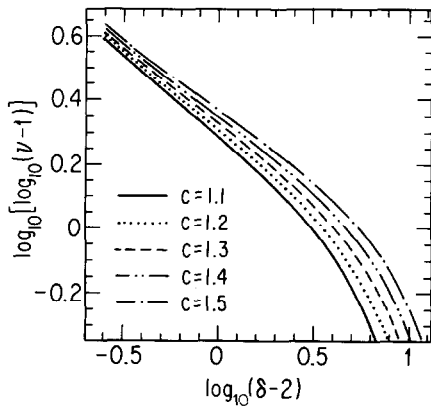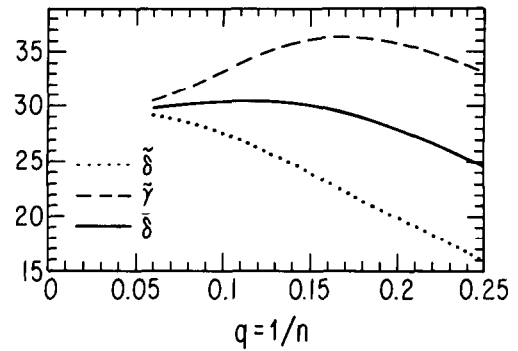

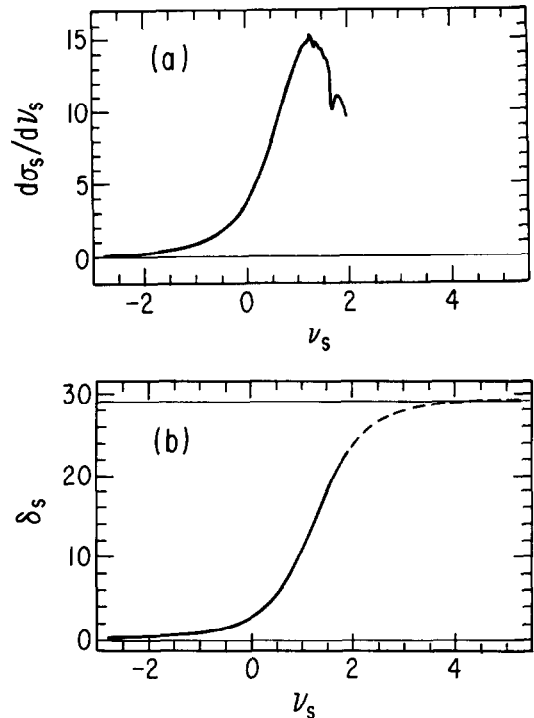Fig. 5. The $\nu \rightarrow \infty$ limit: the inverse Gaussian map.

Fig. 6. The global form of $\delta(\nu)$: (a) δ'_s versus ν_s (see text), (b) δ_s versus ν_s where the continuous line represents the same data as in fig. 3 and the dashed curve is obtained by inverting the low ν data with respect to the point $\nu_s = 1.25$.

Fig. 4. The $\nu \rightarrow 1^+$ limit.

(1) which can be regarded as belonging to the $\nu = \infty$ universality class. In table 1 the values of the ratios $\delta_n(\infty)$ are listed for n between 4 and 18. A slow monotonic convergence to $\delta(\infty) \approx 30$ can be observed. To improve this estimate we define $\tilde{\delta}(q) \equiv \delta_n(\infty)$ where $q = 1/n$ such that $\delta(\infty) = \lim_{q \rightarrow 0} \tilde{\delta}(q)$.

Table 1
The convergence to δ_∞ of $\tilde{\delta}$, $\tilde{\gamma}$ and $\bar{\delta}$ for the inverse Gaussian map (see text and fig. 5).

n	$\tilde{\delta}(1/n)$	$\tilde{\gamma}(1/n)$	$\bar{\delta}(1/n)$
4	15.84423	33.18954	24.51688
5	19.80478	35.79244	27.79861
6	22.49363	36.32217	29.40790
7	24.52404	35.93053	30.22728
8	25.85286	34.96990	30.41138
9	26.84534	34.07744	30.46139
10	27.49777	33.18256	30.34016
11	27.99756	32.50903	30.25330
12	28.33298	31.91092	30.12195
13	28.59962	31.48098	30.04030
14	28.78270	31.10806	29.94538
15	28.93408	30.84240	29.88824
16	29.04016	30.61049	29.82532
17	29.13130	30.44494	29.78812
18	29.19625		

We know that $\tilde{\delta}(q)$ is monotonic, since it converges geometrically for the even and odd subsequences, with a positive factor; for the same reason, the even and odd subsequences are convex, and are intertwined. We then use these facts in the neighborhood of $q=0$ to assure that the value of the limit is bounded between $\tilde{\delta}(q)$ and its Legendre transform $\tilde{\gamma}(q) \equiv \tilde{\delta}(q) - q\tilde{\delta}'(q)$. Moreover, it can be shown, that

$$\bar{\delta}(q) \equiv [\tilde{\delta}(q) + \tilde{\gamma}(q)]/2 = \delta(\infty) + \mathrm{O}(q^3),$$

indicating that $\bar{\delta}(q)$ displays accelerated convergence to the limit (see fig. 5). This procedure leads to the result $\delta(\infty) = 29.8...$ which is in agreement with the analytic estimate made in ref. [9] by means of the renormalization group.

We finally point out an interesting feature in the global form of $\delta(\nu)$. In fig. 6a we show the numerical derivative δ'_s of the function $\delta_s(\nu_s)$ where $\delta_s = \delta - 2$ and $\nu_s = \log(\nu - 1)$. Notice that δ'_s has a maximum at $\nu_s \approx 1.25$ which coincides with the value of c which optimizes the fit to the law of eq. (2). Since our data are poorer as ν increases, the curve δ'_s becomes noisy after this maximum. However, there is evidence suggesting that δ'_s is symmetric around its maximum. On the basis of this hypothesis, we can predict the value of $\delta(\infty)$ using the results from the small ν part

of $\delta(\nu)$. One obtains $\delta(\infty) \approx 31.2$ which is within 5% of the actual value. Accordingly, fig. 6b illustrates the conjectured symmetry of the function $\delta_s(\nu_s)$. A true confirmation of this symmetry should come from the systematic computation of $\delta(\nu)$ for increasing values of $\log(\nu - 1)$. Results of the work in progress on this problem will be discussed elsewhere.

References

[1] M.J. Feigenbaum, J. Stat. Phys. 19 (1978) 25.
[2] M.J. Feigenbaum, J. Stat. Phys. 21 (1979) 669.
[3] N. Metropolis, J.L. Stein and P.R. Stein, J. Comb. Theory 15 (1973) 25.
[4] P. Collet and J.P. Eckmann, Iterated maps on the interval as dynamical systems (Birkhäuser, Basel, 1980).
[5] B. Hu, Phys. Rep. 91 (1982) 233.
[6] J.P. Eckmann and P. Wittwer, Lecture notes in physics, Vol. 227. Computer methods and Borel summability applied to Feigenbaum's equation (Springer, Berlin, 1985).
[7] J.P. van der Weele, H.W. Capel and R. Kluiving, Phys. Lett. A 119 (1986) 15.
[8] J.P. van der Weele, H.W. Capel and R. Kluiving, Physica A 145 (1987) 425.
[9] J.P. Eckmann and H. Epstein, Commun. Math. Phys. 128 (1990) 427.
[10] B. Derrida, A. Gervoise and Y. Pomeau, Ann. Inst. Henri Poincaré 29 (1978) 305.
[11] B. Hu and J.M. Mao, Phys. Rev. A 25 (1982) 3259.
[12] P.R. Hauser, C. Tsallis and E. Curado, Phys. Rev. A 30 (1984) 2074.
[13] D.L. Gonzalez, Ph.D. Thesis, Universidad Nacional de La Plata, La Plata, 1987.
[14] R.W. Hamming, Coding and information theory (Prentice-Hall, Englewood Cliffs, 1986).
[15] B.-L. Hao, Elementary symbolic dynamics and chaos in dissipative systems (World Scientific, Singapore, 1989).